

ROSENHAHNITE,<sup>1</sup> A NEW HYDROUS CALCIUM SILICATE  
FROM MENDOCINO COUNTY, CALIFORNIA

A. PABST, *Dept. of Geology and Geophysics, University of  
California, Berkeley, California*

AND E. B. GROSS, J. T. ALFORS, *California Division of Mines  
and Geology, San Francisco, California.*

ABSTRACT

Rosenhahnite, a new hydrous calcium silicate, forms narrow veins in brecciated, fine-grained diopside-garnet metasedimentary rock in Mendocino County, California. It is colorless to buff and in cavities forms etched, lath-like crystals up to 5 mm in maximum dimension. The crystals are triclinic, and {010} is invariably the principal form. Cleavages are {001} perfect, {100} and {010} good. Hardness is 4.5-5. Refractive indices are  $\alpha = 1.625$ ,  $\beta = 1.640$ ,  $\gamma = 1.646$ ; 2V measured by universal stage is  $-64 \pm 4^\circ$ .

The formula is  $(\text{CaSiO}_3)_3 \cdot \text{H}_2\text{O}$  with minor substitution of Ba for Ca.

The cell dimensions, are  $a = 6.946$ ,  $b = 9.474$ ,  $c = 6.809$ , all  $\pm 0.006$  Å,  $\alpha = 108^\circ 39'$ ,  $\beta = 94^\circ 49'$ ,  $\gamma = 95^\circ 43'$ ;  $Z = 2$ , density (calc.) 2.905, (meas.)  $2.89 \pm 0.02$ . Morphological evidence does not permit a choice between space groups  $P\bar{1}$  and  $P1$ .

Rosenhahnite loses water very slowly between 400-500°C. Single crystals of rosenhahnite are covered to single crystals of triclinic wollastonite in perfect topotactic relation. There is no indication of formation of intermediate phases, even though the composition of xonotlite lies between those of rosenhahnite and wollastonite.

Rosenhahnite is the natural counterpart of a phase reported by Pistorius (1963) to be stable at temperatures below about 450°C and at H<sub>2</sub>O pressures above about 20 kilobars.

INTRODUCTION

In late 1962, Leo Rosenhahn, an amateur mineralogist, found a mineral in veinlets within boulders in the streambed of the Russian River, five miles north of Cloverdale in Mendocino County, California. The material was identified as tilleyite after a cursory X-ray examination by U. S. Army Corps Engineers Laboratory, Sausalito, California. In early 1965 Rosenhahn submitted specimens to the California Division of Mines and Geology for further study since his optical values did not agree with those for tilleyite. A careful optical and X-ray diffraction investigation and spectrographic analysis indicated that the crystalline material was a new hydrous calcium silicate.

The mineral is named for Mr. Rosenhahn, San Anselmo, Marin County, California, and the authors greatly appreciate his assistance in furnishing specimens for study and showing one of the authors (E. B. Gross) the location of the float material.

<sup>1</sup> The name has been approved by the Commission on New Minerals and Mineral Names, International Mineralogical Association.

## OCCURRENCE

Rosenhahnite is primarily a vein-forming mineral in dark gray boulders, one to three feet in diameter, along the east bank of the Russian River adjacent to U. S. Highway 101, five miles north of Cloverdale, California. The locality is 1.8 miles north of the Mendocino County-Sonoma County line near the center of E 1/2, E 1/2, Sec. 23, T.12N., R.11 W., as shown on the Cloverdale, California 7 1/2 minute topographic quadrangle (1960).

Narrow veinlets less than 3 cm thick of buff to white, massive rosen-

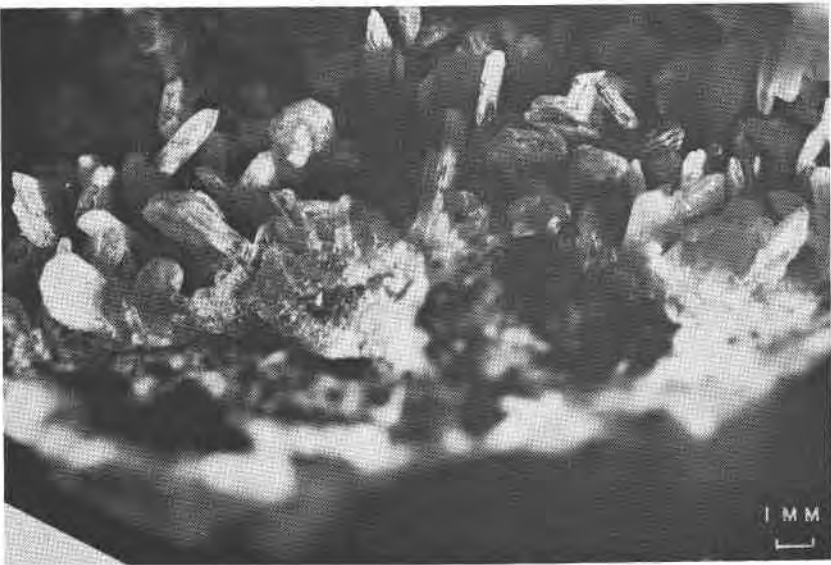


FIG. 1. Crystals of rosenhahnite.

hahnite transect brecciated, fine-grained metasedimentary rock in which the original sedimentary textures are preserved. Occasionally open spaces up to 8 mm in cross-section within the buff-colored veinlets contain clear as well as etched, flat tabular crystals of rosenhahnite (Fig. 1). One specimen contains hollow opal pseudomorphs after rosenhahnite. Some white massive veinlets consist of a mixture of rosenhahnite, pectolite, and xonotlite; others contain rosenhahnite, diopside, garnet and calcite. The calcite partially replaces rosenhahnite and diopside. Usually the habit and glistening of the cleavages of rosenhahnite in sunlight enables one to distinguish it from the associated acicular pectolite and xonotlite. Some veinlets of rosenhahnite have been displaced by younger

microfaults and calcite-filled veinlets. The dense, gray host-rock is composed of fine-grained diopside with variable amounts of hydrogrossular ( $a = 11.93 \text{ \AA}$ ), finely fibrous aggregates of tremolite, and minor sphene. Specimens may also contain rosenhahnite in the matrix and rare unidentified black organic material.

Xonotlite occurs as radial acicular aggregates intergrown with rosenhahnite, but the relative ages of the two minerals could not be determined. Crystals of acicular pectolite and equidimensional datolite are attached to crystals of rosenhahnite in cavities and appear to be later than rosenhahnite. A 0.5 mm-thick veinlet of datolite was found cutting veinlets of rosenhahnite in one specimen.

All attempts to locate the source outcrops of the rosenhahnite-bearing boulders have been unsuccessful. About 10 boulders containing rosenhahnite found to date were rounded and some had a chalky white alteration of opal-like material and calcite developed on the pectolite and xonolite.

The bedrock in the vicinity of the rosenhahnite locality is a greenish gray, medium- to coarse-grained sandstone which is composed essentially of quartz, albite, and chlorite with veins of quartz and calcite. Leonhardtite coats fractures in some outcrops. This sandstone is in tectonic contact with altered diabase composed of augite, altered plagioclase, chlorite, and quartz with veins of radiating buff prehnite and quartz. Locally breccia zones up to one foot thick occur along the contact between the sandstone and diabase.

Other rocks in the vicinity include serpentine, chert, hard black shale, and blocks of glaucophane schist all of which contain numerous veinlets, mainly of quartz and calcite, but some rocks also contain veinlets of pectolite, xonolite, datolite, and apophyllite. The restricted distribution of the rosenhahnite-bearing boulders suggest that the boulders may be derived locally.

#### MORPHOLOGY

The crystals occur in irregular clusters and are mostly dull and etched. Eleven were selected from one hand specimen for measurement by 2-circle goniometer. Only one of these was doubly terminated; all others were broken off on a basal cleavage. Seven of the 10 singly-terminated crystals showed faces with  $l$  positive. The number of faces identified on each crystal varied from 10 to 21. The crystals are somewhat unevenly developed and no decision as to the presence or absence of a center of symmetry could be made on the basis of morphology. The faces of the principal forms occur mostly in centrosymmetrical pairs but many of the minor forms are usually represented by only one face. Excluding  $a$ ,  $b$  and  $c$ , 27

$hk0$ ,  $10\ 0kl$ ,  $3\ h0l$  and  $15\ hkl$  forms were identified, the latter mostly represented by only a single observation. Many narrow, dull or etched faces, especially numerous in the  $hk0$  and  $0kl$  zones, could not be identified. The order of prominence of the principal forms is suggested in Table 1 in the column in which the number of observations for each is recorded. The angles given in the table are based on axial elements calculated from the X-ray data.

The crystals are always tabular to lath-like with  $\{010\}$  by far the most prominent form. Figure 2 shows idealized views of the positive and nega-

TABLE 1. STANDARD ANGLE TABLE FOR ROSENHAHNITE

$$a:b:c=0.7332:1:0.7187 \quad \alpha\ 108^\circ 39' \quad \beta\ 94^\circ 49' \quad \gamma\ 95^\circ 43'$$

$$p_0:q_0:r_0=0.9334:0.7201:1 \quad \lambda\ 70^\circ 41', \mu\ 82^\circ 56', \nu\ 82^\circ 17'$$

$$p_0'=0.9925, q_0'=0.7657, x_0'=0.0843, y_0'=0.3515$$

Number of observations	Forms	$\phi$	$\rho$	<i>A</i>	<i>B</i>	<i>C</i>
9	<i>c</i> 001	13° 29'	19° 52'	82° 56'	70° 41'	— —
20	<i>b</i> 010	0 00	90 00	82 17	— —	70 41
16	<i>a</i> 100	82 17	90 00	— —	82 17	82 56
4	<i>k</i> 140	17 06	90 00	65 11	17 06	70 08
4	<i>m</i> 110	47 34	90 00	34 43	47 34	73 38
4	<i>n</i> 210	62 19	90 00	19 58	62 19	77 03
7	<i>M</i> $\bar{1}10$	122 44	90 00	40 27	122 44	96 28
4	<i>N</i> $\bar{2}10$	104 14	90 00	21 57	104 14	90 16
3	<i>u</i> $0\bar{3}2$	173 58	38 42	91 03	128 55	58 14
3	<i>v</i> $0\bar{2}1$	175 55	49 47	92 46	139 37	68 56
3	<i>w</i> $0\bar{3}1$	177 31	63 05	94 40	152 58	82 17
5	<i>D</i> $\bar{1}01$	—76 22	42 47	129 14	80 16	46 18
2	<i>Q</i> $\bar{1}22$	—139 42	32 12	115 12	113 59	50 38

tive ends of two crystals bounded at the opposite ends by basal cleavages in typical fashion.

#### PHYSICAL AND OPTICAL PROPERTIES

The more or less lath-like crystals of rosenhahnite are elongated parallel to *c*, flattened parallel to  $\{010\}$  and break along  $\{001\}$  cleavage and less commonly on  $\{100\}$  and  $\{010\}$ . The crystals attain a maximum size of  $5 \times 2 \times 1$  mm. Crystals have a hardness of 4.5–5 and density of  $2.89 \pm 0.02$ , measured on a Berman balance. The density calculated from the ideal formula,  $2[\text{Ca}_3\text{Si}_3\text{O}_9 \cdot \text{H}_2\text{O}]$ , is 2.905. Rosenhahnite is only slightly soluble in concentrated acids.

The refractive indices are  $\alpha = 1.625 \pm 0.002$ ,  $\beta = 1.640 \pm 0.002$ , and

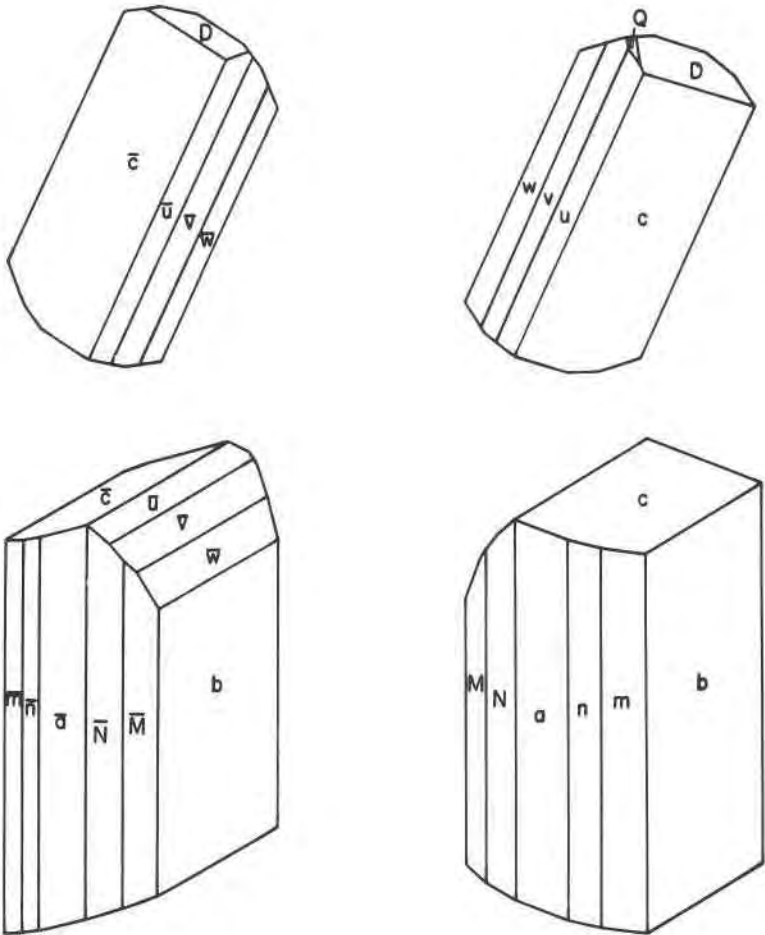


FIG. 2. Idealized drawings of rosenhahnite.  $c$  upward in drawing at right,  $\bar{c}$  upward in drawing at left. The lower drawings are axonometric projections, the normal to the plane of projection being defined by  $\phi$   $65^\circ$ ,  $\rho$   $80^\circ$ . The lettering corresponds to that used in Table 1.

$\gamma = 1.646 \pm 0.002$  measured in sodium light. The birefringence is 0.021 and the axial angle measured by universal stage is  $-64 \pm 4^\circ$ . The calculated axial angle is  $-64$  degrees.

The optical orientation of rosenhahnite was determined by universal stage on four grains separately mounted in balsam and three large favorably oriented crystals in thin section. The average values from the seven determinations are given below. The figures for  $Z$  in parentheses are adjusted for consistency with  $X$  and  $Y$ . A wholly independent deter-

mination by an extinction curve method was carried out on a crystal whose orientation was determined by X-ray and goniometric measurements. The determinations by both methods are in excellent agreement.

The orientations are:

	Average of 7 universal stage determinations		Determination on a single crystal by extinction curves	
	$\phi$	$\rho$	$\phi$	$\rho$
X	$-99^\circ$	$72^\circ$	$-99^\circ$	$72^\circ$
Y	$1^\circ$	$64^\circ$	$2^\circ$	$65^\circ$
Z	$139^\circ$ ( $141^\circ$ )	$34^\circ$ ( $33^\circ$ )	$142^\circ$	$33^\circ$

The extinction angles as seen when fragments are lying on (001), (100) and (010) faces are given below:

Lying on		Observed	Constructed
(001)	$\gamma'$ to trace of (100)	$7\frac{1}{2}^\circ$	$8^\circ$
(100)	$\gamma'$ to trace of (001)	$36^\circ$	$35^\circ$
(010)	$\alpha'$ to trace of (001)	$15^\circ$	$14^\circ$

A plot of the optical orientation is given in Figure 3. Physical and optical properties of rosenhahnite are compared with xonotlite and wollastonite in Table 2.

The mean index of refraction calculated by the rule of Gladstone and Dale (Larsen and Berman, 1934, p. 31) from the recalculated analysis (Table 3, Column D) and the measured density (2.89) is 1.639. The mean

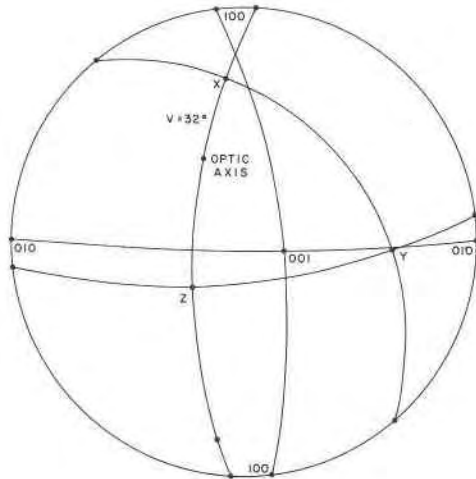


FIG. 3. Stereographic projection showing optical orientation of rosenhahnite.

TABLE 2. PHYSICAL, OPTICAL, AND UNIT-CELL DATA OF ROSENHAHNITE COMPARED WITH XONOTLITE AND WOLLASTONITE

	Rosenhahnite	Xonotlite	Wollastonite
Composition	$\text{Ca}_3\text{Si}_2\text{O}_9 \cdot \text{H}_2\text{O}$	$\text{Ca}_6\text{Si}_6\text{O}_{17}(\text{OH})_2$	$\text{CaSiO}_3$
System	Triclinic	A-centered geometrically or orthorhombic	Triclinic
Refractive indices	$\alpha = 1.625$ $\beta = 1.640$ $\gamma = 1.646$	1.583 1.583 1.595	1.620 1.632 1.634
Birefringence	0.021	0.012	0.014
Optic sign, 2V	(-), $64^\circ$	(+), low	(-), $39^\circ \pm 3^\circ$
Hardness	4, 5-5	6.0	4, 5-5
References optics	This report	Larsen (1923)	Heller and Taylor (1956)
Cell dimensions	$a$ $6.946 \pm 0.006 \text{ \AA}$ $b$ $9.474 \pm 0.006 \text{ \AA}$ $c$ $6.809 \pm 0.006 \text{ \AA}$ $\alpha = 108^\circ 39'$ $\beta = 94^\circ 49'$ $\gamma = 95^\circ 43'$	17.10 7.34 14.06	7.94 7.32 7.07 $90^\circ 02'$ $95^\circ 22'$ $103^\circ 20'$
Cell content	2	4	2
Volume of cell ( $\text{\AA}^3$ )	418.96	1764.73	398.1
$\text{\AA}^3/\text{oxygen atom}$	20.95	23.22	22.12
Measured density	$2.89 \pm 0.02$	2.71	2.88
Calculated density	2.905	2.69	2.906
Space group	$P\bar{1}$ or $P1$		$P1$
References	This report	Taylor (1964),	Jeffery in Taylor
X-ray data		2, 376	(1964), 1, 139

index of refraction calculated from the ideal composition and the measured density is 1.641. The measured mean index of refraction  $(\alpha + \beta + \gamma)/3$  is 1.637.

#### X-RAY CRYSTALLOGRAPHY

The direct cell dimensions for rosenhahnite were obtained from measurements on five quartz-calibrated Weissenberg patterns for the three principal zones, made with three crystals especially selected for this purpose.

Unit cell data and other values for rosenhahnite are compared with similar data for xonotlite and wollastonite in Table 2. Material has been supplied to Dr. J. W. Jeffery of Birkbeck College for determination of the crystal structure of rosenhahnite.

TABLE 3. ANALYSIS OF ROSENHAHNITE FROM MENDOCINO COUNTY, CALIFORNIA

	A	B	C	D	E
SiO <sub>2</sub>	47.0		47.0	48.61	49.18
Al <sub>2</sub> O <sub>3</sub> <sup>1</sup>	0.06		0.06	0.06	
TiO <sub>2</sub>	nil		nil	nil	
FeO <sup>2</sup>	0.17		0.17	0.18	
MnO	0.006		0.006	0.006	
MgO	0.1		< 0.1	0.10	
CaO <sup>3</sup>	45.0		43.34	44.83	45.90
Na <sub>2</sub> O	0.2		0.2	0.21	
K <sub>2</sub> O <sup>4</sup>	nil		nil	nil	
BaO	0.75		0.75	0.77	
SrO	0.03		0.03	0.03	
B <sub>2</sub> O <sub>3</sub> <sup>5</sup>	0.001		0.001	0.001	
Ign. Loss	6.5 <sup>6</sup>	5.2 <sup>7</sup>	5.2	5.2	4.92
Total	99.82		96.86	100.00	100.00

<sup>1</sup> Al<sub>2</sub>O<sub>3</sub> possibly contamination from mullite mortar.

<sup>2</sup> Determined as Fe, but reported FeO. May include some impurity from plattner mortar.

<sup>3</sup> Includes CaO from 2.96% CaCO<sub>3</sub> impurity.

<sup>4</sup> K<sub>2</sub>O determined by x-ray spectroscopy on a separate split of sample.

<sup>5</sup> B<sub>2</sub>O<sub>3</sub> determined on a separate split of sample.

<sup>6</sup> Ignition loss of 950°C on a separate 10 mg split of sample; includes CO<sub>2</sub> from 2.96% CaCO<sub>3</sub> impurity.

<sup>7</sup> Ignition loss made by A. Pabst on a separate 1 gm sample.

Column A is the uncorrected emission spectrograph analysis. The sample contained 2.96% CaCO<sub>3</sub> impurity. Portions were split from an original 100 mg sample. Analysed by J. T. Alfors.

Column B is the ignition loss on a 1 gm sample determined by A. Pabst. during a dehydration run.

Column C is the spectrographic analysis of column A after subtracting 1.3% CO<sub>2</sub> from the ignition loss result of 6.5%, 1.66% CaO (the equivalent CaO to correspond with CO<sub>2</sub> to make calcite; a total of 2.96% CaCO<sub>3</sub>).

Column D is the spectrographic analysis (C) recalculated to 100%. The ignition loss amounting to 5.2% H<sub>2</sub>O was held constant in this calculation. Values are accurate to two significant figures only.

Column E is the ideal composition calculated from the formula 2[Ca<sub>3</sub>Si<sub>3</sub>O<sub>9</sub>·H<sub>2</sub>O].

#### CHEMICAL ANALYSIS

Rosenhahnite was analyzed by d-c arc emission spectroscopy utilizing a borate fusion technique described by Joensuu and Suhr (1962). The mineral, powdered in a mullite mortar, was fused in five parts by weight of lithium tetraborate and one part lithium tetraborate which contained approximately seven percent Co<sub>3</sub>O<sub>4</sub> as an internal standard. The resulting borate beads were crushed in a Plattner mortar, ground in a boron carbide



mortar, and mixed with two parts of graphite. Two  $\frac{1}{8}$  inch-diameter graphite electrodes were each loaded with a charge that included the equivalent of about 3 mg of mineral and were burned to completion with a Stallwood jet in carbon dioxide.

Another d-c arc emission spectrographic analysis was made of a split of the sample to check for boron and lithium. For the second spectrographic analysis the powdered sample was mixed with two parts graphite, loaded in two  $\frac{1}{8}$  inch-diameter graphite electrodes and burned to completion with a Stallwood jet in carbon dioxide. The results of the second spectrographic analysis are only semiquantitative but the  $B_2O_3$  content was estimated to be 0.001 percent and no lithium could be detected. Potassium was checked by X-ray fluorescence but none was detected.

The results of the two emission spectrographic analyses and one ignition loss determination are presented in Table 3, Column A. Pabst ran a dehydration curve on one gram of pure rosenhahnite and obtained a weight loss of 5.2 percent (Table 3, Column B). The 1.3 percent difference in the ignition losses is assigned to  $CO_2$  from calcite impurity in the spectrographically analyzed material. Column C, of Table 3, is the analysis of Column A less  $CaO$  and  $CO_2$  equivalent to 2.96 percent calcite impurity. The analysis recalculated to 100 percent is given in Table 3, Column D. The ideal composition based on the formula  $Ca_3Si_3O_9 \cdot H_2O$  is given in Column E of Table 3. As a check on the emission spectrographic analysis Robert Jack, University of California, analyzed the material used for the weight loss curve by X-ray spectroscopy utilizing pure wollastonite and dehydrated xonotlite as standards. The X-ray spectrographic analysis confirmed the 1:1 ratio of  $CaO$  to  $SiO_2$ .

The cell content, calculated from the analysis in Table 3, Column D, the measured density (2.89), and the cell volume listed in Table 2, is  $(Ca_{5.83}Na_{0.05}Ba_{0.04}Mg_{0.02}Fe_{0.02})(Si_{5.90}Al_{0.01})O_{17.75} \cdot 2.10H_2O$ . This reduces to  $2[(Ca,Na,Ba,Mg,Fe)_{2.96}(Si,Al)_{2.96}O_{8.88} \cdot 1.05H_2O]$  which can be simplified to  $2[Ca_3Si_3O_9 \cdot H_2O]$ .

#### CHANGES UPON HEATING

Figure 4 shows dehydration data for rosenhahnite obtained by repeated heating and weighing of a pure one-gram sample. The period of heating at each temperature varied from 4 to 56 hours. At  $420^\circ C$  constant weight was not attained but the rate of weight loss at the end of 51 hours was only about 0.003%/hour, and at  $540^\circ C$  the rate at the end of 56 hours was about 0.001%/hour. Up to some temperature between  $335^\circ$  and  $420^\circ C$  there is no weight loss. Most of the weight loss occurred in the heatings at  $420^\circ$  and  $540^\circ C$  but the rate of loss at those tempera-

tures is very low even for powdered material. Along with the powdered rosenhahnite, numerous single crystals were heated to various temperatures. Several of these were examined microscopically, by reflecting goniometer and by X-ray diffraction both before and after heating. Crystals heated to complete dehydration (weight loss about 5.2%) are changed to single crystals of triclinic  $\beta$ -CaSiO<sub>3</sub> (wollastonite) having the cell dimensions reported in Taylor (1964) and showing very faintly the reciprocal lattice rods parallel to  $a^*$ , for  $hkl$  with  $k$  odd, described by Jeffery (1953).

The newly formed wollastonite is in perfect topotactic relation to the parent rosenhahnite. This was established by single crystal X-ray examination of several crystals that had been partly converted. No evidence

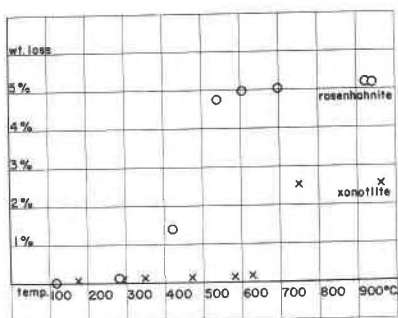


FIG. 4. Dehydration data for rosenhahnite and xonotlite.  
See text for experimental conditions.

for any intermediate phases was found, though the composition of xonotlite is intermediate between those of rosenhahnite and wollastonite. Crystals heated to 420°C in accordance with the scheme indicated in Figure 4 are specially suited for study of the conversion. Such crystals yield diffraction patterns of the original rosenhahnite practically undisturbed and superposed on these single crystal patterns of wollastonite always in a fixed relation. Figure 5 shows an  $a$ -axis precession pattern of a rosenhahnite crystal heated to 420°C. It shows the full complement of rosenhahnite  $0kl$  spots plus all but the weakest  $hk0$  spots of wollastonite only slightly less sharp. The partial coincidence of the two reciprocal lattices is shown in Figure 6, which can be matched with the precession pattern. By means of sets of such patterns for each of several partly converted crystals the orientation relations of the two lattices were established. Some particular lattice correspondences are summarized in Table 4. In the following discussion subscripts  $r$  and  $w$  are used to identify lattice elements of the two phases.

The stereographic projection, Figure 7, is drawn on the assumption that the reciprocal lattice planes in Figures 5 and 6 coincide exactly. The lack of parallelism of lattice rows belonging in these superposed planes then need not exceed  $0^{\circ}22\frac{1}{2}'$ , the difference between  $\alpha_r^*$ ,  $70^{\circ}41'$ , and  $(\bar{1}10) \wedge (120)_w$ ,  $71^{\circ}3\frac{1}{2}'$ . If  $(\bar{1}10)_w$  coincides with  $(001)_r$ , then the departure of  $[110]_w$  from  $b_r$  would be  $2^{\circ}33'$ , the difference between  $\gamma_r$ ,  $95^{\circ}43'$  and

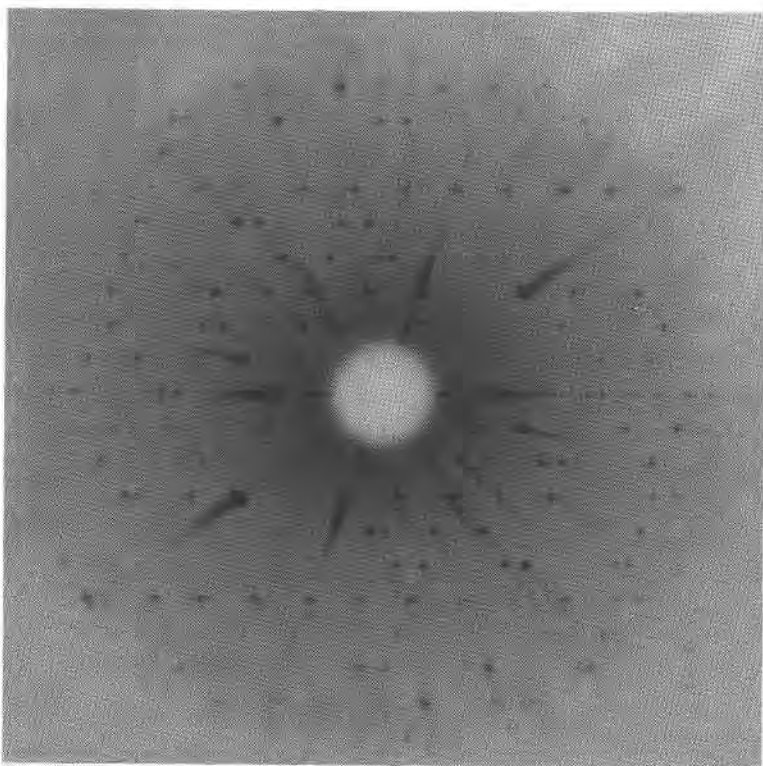


FIG. 5. *a*-axis precession pattern of rosenhahnite after heating to  $420^{\circ}\text{C}$ . Shows triclinic wollastonite spots.  $\mu = 22$ ; Mo-Zr radiation for 20 hours. Compare figure 6.

$(c \wedge [110])_w$ ,  $93^{\circ}10'$ . If the nearly coincident  $(h0l)_r$  and  $(\bar{h}hl)_w$  reciprocal lattice parameters are seen in a single pattern with  $(00l)_r$  coincident with  $(hh0)_w$  then  $(h00)_r$  should be offset from  $(00l)_w$  by  $11^{\circ}34'$ , the difference between  $97^{\circ}4'$ , the supplement of  $\beta_r^*$ , and  $85^{\circ}30'$ ,  $(\bar{1}10) \wedge (00\bar{1})_w$ . Direct measurement of the angle on a precession pattern gave  $11^{\circ}30' \pm 10'$  and it was seen to be about  $12^{\circ}$  on several Weissenberg patterns.

Coincidence of  $c_w$  with  $a_r$  and of  $(110)_w$  with  $(001)_r$  has been assumed. However, it may seem more probable that  $[110]_w$  coincides exactly with

$b_r$ . In that case  $c_{10}$  must be at least  $2^\circ 33'$  from  $a_r$ . Possibly some intermediate orientation is assumed or the lattices may be slightly distorted by the influence of one upon the other, as has been suggested for certain coexistent feldspar lattices. Precession and Weissenberg patterns may not be adequate to resolve such questions as the effects would correspond to those produced by missettings of the order of  $1\frac{1}{4}^\circ$  or less.

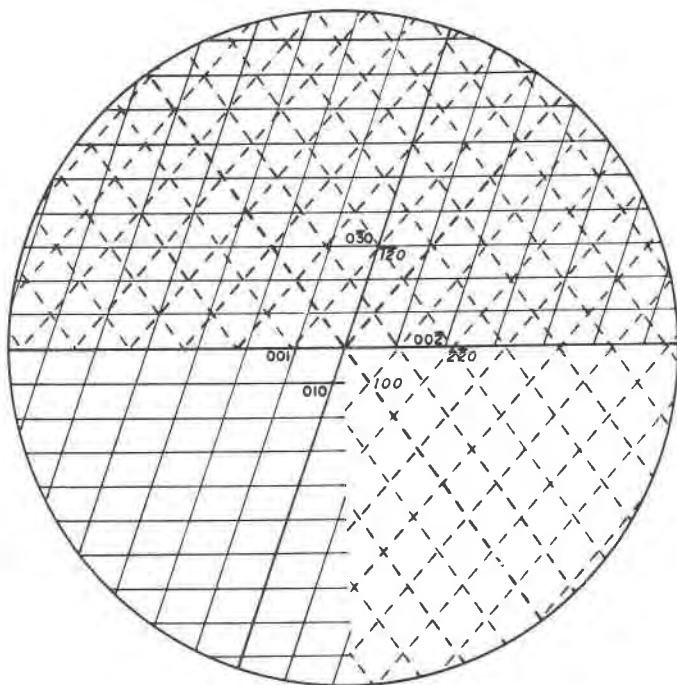


FIG. 6.  $OkI$  reciprocal lattice plane of rosenhahnite in solid lines, vertical indices.  $hkO$  reciprocal lattice plane of triclinic wollastonite in dashed lines, slanting indices. Scale matches Figure 5. The overlap of lattices in upper part of drawing corresponds to the dual pattern reproduced in Figure 5.

Thermal dehydration data were also obtained on one gram of xonotlite from Army Street, San Francisco, and are included in Figure 4. The dehydration occurs at a higher temperature than in rosenhahnite but is more rapidly completed. There is only a trifling weight loss at  $625^\circ\text{C}$ , but dehydration is complete in 14 hours or less at  $750^\circ\text{C}$ . Similar data on the dehydration of xonotlite, obtained by P. G. Nutting, were published by Schaller (1950, Fig. 1). A single crystal of xonotlite, dehydrated at this temperature and rotated on the original  $b$  axis, yielded an X-ray powder

TABLE 4. SOME LATTICE CORRESPONDENCES BETWEEN ROSENHAHNITE AND TOPOTACTICALLY FORMED WOLLASTONITE

Rosenhahnite		Wollastonite	
<i>a</i>	6.942 Å	<i>c</i>	7.07
<i>d</i> (030)	2.960	<i>d</i> (120)	2.979
<i>d</i> (002)	3.198	<i>d</i> (220)	2.979
<i>b</i>	9.445 Å	[110]	9.445
<i>d</i> (100)	6.860	<i>d</i> (001) <sup>1</sup>	7.037
$\gamma$	95°43'	$c \wedge [110]$	93°10'
$\alpha^*$	70°41'	(120) $\wedge$ ( $\bar{1}10$ )	71°3½'

<sup>1</sup> See text.

pattern of wollastonite with some preferred orientation and superposed on this a weak but perfect *b* axis rotation pattern of wollastonite, confirming the results of Dent and Taylor (1956), who used material from the same locality and found that "a single crystal of xonotlite dehydrates to a single crystal of  $\beta$ -CaSiO<sub>3</sub>, together with varying amounts of unoriented or partly oriented material." It is surprising that the topotaxy of  $\beta$ -CaSiO<sub>3</sub> formed from rosenhahnite is so much more perfect even though

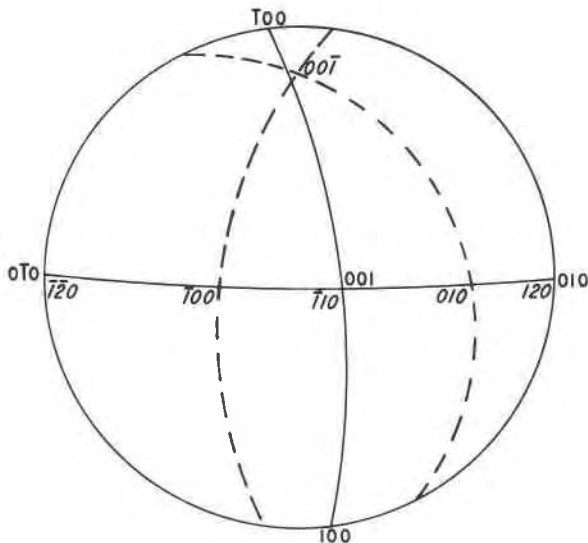


FIG. 7. Stereographic projection showing the relation of the wollastonite lattice to the rosenhahnite lattice as it arises from topotactic transformation. Solid lines and vertical indices refer to rosenhahnite, dashed lines and slanting indices to wollastonite. The *hkl* zone of wollastonite is shown in exact coincidence with the *Okl* zone of rosenhahnite.

a greater change in composition is involved. Material has been supplied to Professor Taylor for a study of the mechanism of the thermal transformation of rosenhahnite.

Crystals of rosenhahnite which are converted or partly converted to wollastonite retain their shape. There is no visible cracking and interfacial angles change little, if at all, though the crystals become opaque and porcelaneous. Though no longer clear so that conoscopic observations are impossible, thin edges of the converted crystals permit refractive index observations. In fully converted crystals the mean index is near 1.60,  $\gamma' = 1.608$  in some, and the birefringence is reduced while there is marked change in extinction directions. The refractive indices of  $\beta$ -CaSiO<sub>3</sub> formed from xonotlite are similar to those of  $\beta$ -CaSiO<sub>3</sub> formed from rosenhahnite,  $\gamma'$  also being close to 1.608.

A decrease in density of the order of 5 percent accompanies the topotactic transformation. This was noted on several crystals. The best observations were obtained on a fragment initially weighing 22.68 mg. Its density of 2.89 changed to 2.73 after a weight loss of 5.25 percent upon heating at 935°C for seven hours. Immediate reweighing after drying off the surficial toluene (in which the crystal was immersed during the Berman balance observations) showed that the sample had not absorbed any toluene and so presumably had no pores accessible to this liquid. The values for the cell volumes and volumes per oxygen atom for rosenhahnite, xonotlite and wollastonite, given in Table 2, may be noted in this connection.

Combining observations on changes in refractive indices and density with X-ray results suggests that the single crystals of wollastonite formed topotactically from rosenhahnite must include about 5 percent voids not directly visible. The low refractive indices observed are those of the aggregate of crystal and voids and have about the expected value.

#### X-RAY POWDER DATA

X-ray powder data of rosenhahnite are given in Table 5. The indexing has been carried only as far as the limit of spacing calculations. Calculated spacings are given only for observed lines. The indexing was checked completely by comparison with appropriate Weissenberg and precession patterns.

#### SYNTHETIC PHASE

Pistorious (1963) reported a new phase formed below 450°C and at H<sub>2</sub>O pressures higher than those at which xonotlite is formed, pressures of the order of 20 kilobars or more. Concerning this phase he writes: "It is very probable that the new phase is either a high-pressure poly-

TABLE 5. X-RAY POWDER DATA OF ROSENHAHNITE,  $\text{Ca}_3\text{Si}_3\text{O}_9 \cdot \text{H}_2\text{O}$ , COMPARED WITH VALUES OF A SYNTHETIC PHASE OF PISTORIUS

<i>hkl</i>	Rosenhahnite			Synthetic	
	<i>d</i> , Å (calc.)	<i>d</i> , Å (obs.)	<i>I</i>	<i>d</i> Å	<i>I</i>
010	8.890	8.90	10		
100	6.859	6.80	5		
1 $\bar{1}$ 0	5.821	5.81	15		
110	5.110	5.11	7	5.09	17
1 $\bar{1}$ 1	4.589	4.56	10		
011	4.532				
020	4.445	4.47	5		
1 $\bar{1}$ 1	4.098	4.10	7		
120	3.983	3.99	15		
1 $\bar{2}$ 1	3.623	3.62	5	3.619	13
111	3.547	3.53	5		
120	3.522				
200	3.430	3.43	25		
2 $\bar{1}$ 0	3.356	3.36	30	3.351	30
002	3.201	3.20	100	3.198	100
1 $\bar{1}$ 2	3.140	3.137	20		
0 $\bar{2}$ 2	3.136				
0 $\bar{3}$ 1	3.110	3.043	60		
210	3.064				
2 $\bar{1}$ 1	3.043	2.965	90	3.040	35
2 $\bar{1}$ 1	2.966				
030	2.963	2.880	15	2.961	80
1 $\bar{2}$ 2	2.881				
201	2.880	2.825		2.871	20
122	2.825				
102	2.774	2.819	5	2.826	30
2 $\bar{1}$ 1	2.769	2.775	40		
032	2.668	2.659	30		
221	2.643				
220	2.555	2.549	15		
211	2.551				
221	2.545	2.512	5		
2 $\bar{1}$ 2	2.513				
202	2.499	2.414	20d		
112	2.423				
230	2.408				
031	2.403				
231	2.403				

Many more lines not measured.

*d*(obs.) as measured on film from 114.59 mm Norelco camera with Cu-Ni radiation, exposed in line position. All lines are also observed on film exposed with Cr-V radiation, on which line marked (#) was resolved.

Intensities were estimated with a photographic scale of graded exposures. Pistorius used Co-Fe radiation.

TABLE 5—(Continued)

<i>hkl</i>	Posenhahnite			Synthetic	
	<i>d</i> , Å (calc.)	<i>d</i> , Å (obs.)	<i>I</i>	<i>d</i> Å	<i>I</i>
		2.353	5	2.343	10
		2.315	10	2.304	13
		2.295	25	2.291	20
		2.251	15	2.252	17
		2.203	20	2.203	10
		#2.183	5		
		2.166	20	2.164	20
		2.133	6		
		2.093	5		
		2.076	5		
		2.044	5		
		1.998	8		
		1.974	10	1.976	13
		1.926	10d		
		1.886	30	1.886	17
		1.862	8		

morph of xonotlite, or else a compound with the formula  $\text{CaSiO}_3 \cdot x\text{H}_2\text{O}$  where  $1 > x > 1/5$ ." The composition of rosenhahnite is in the stated range. The powder diffraction data reported by Pistorius for this phase are shown in Table 5 alongside the data for rosenhahnite. There can be little doubt that the phase is the synthetic equivalent of rosenhahnite.

## REFERENCES

- DENT, L. S. AND H. F. W. TAYLOR (1956) The dehydration of xonotlite. *Acta Crystallogr.* **9**, 1002-1004.
- GARD, J. A. (1962) Interpretation of weak reflections in electron diffraction patterns. *Proc. Eur. Reg. Conf. Electron Microsc.*, Delft, 1960, **1**, 203-206.
- HELLER L. AND H. F. W. TAYLOR (1956) *Crystallographic data for the calcium silicates*. His Majesty's Stationery Office, London, 79p.
- JEFFERY, J. W. (1953) Unusual x-ray diffraction effects from a crystal of wollastonite. *Acta Crystallogr.* **6**, 821-825.
- JOENSUU, O. I. AND N. H. SUHR (1962) Spectrochemical analysis of rocks, minerals, and related materials. *Appl. Spectrosc.* **16**, 101-104.
- LARSEN, E. S. (1923) The identity of eakleite and xonotlite. *Amer. Mineral.* **8**, 181-182.
- LARSEN, E. S. AND HARRY BERMAN (1934) The microscopic determination of the nonopaque minerals. *U.S. Geol. Surv. Bull.* **848**, 31.
- PISTORIUS, C. W. F. T. (1963) Thermal decomposition of portlandite and xonotlite to high pressure and temperatures. *Amer. J. Sci.* **261**, 79-87.
- SCHALLER, WALDEMAR T. (1950) Miserite from Arkansas; a renaming of natroxonotlite. *Amer. Mineral.* **35**, 911-921.
- TAYLOR, H. F. W. (1964) *The Chemistry of Cements* Academic Press, New York, 2 vols.

*Manuscript received, May 16, 1966; accepted for publication, July 25, 1966.*